

---

# Detecting Brittle Decisions for Free: Leveraging Margin Consistency in Deep Robust Classifiers

---

**Jonas Ngawé**

IID-Université Laval and Mila  
jonas.ngawe.1@ulaval.ca

**Sabyasachi Sahoo**

IID-Université Laval and Mila  
sabyasachi.sahoo.1@ulaval.ca

**Yann Pequignot**

IID-Université Laval  
yann.pequignot@iid.ulaval.ca

**Frédéric Precioso**

Université Côte d’Azur, CNRS, INRIA, I3S, Maasai  
frederic.precioso@univ-cotedazur.fr

**Christian Gagné**

IID-Université Laval, Mila and Canada CIFAR AI Chair  
christian.gagne@gel.ulaval.ca

## Abstract

Despite extensive research on adversarial training strategies to improve robustness, the decisions of even the most robust deep learning models can still be quite sensitive to imperceptible perturbations, creating serious risks when deploying them for high-stakes real-world applications. While detecting such cases may be critical, evaluating a model’s vulnerability at a per-instance level using adversarial attacks is computationally too intensive and unsuitable for real-time deployment scenarios. The input space margin is the exact score to detect non-robust samples and is intractable for deep neural networks. This paper introduces the concept of margin consistency – a property that links the input space margins and the logit margins in robust models – for efficient detection of vulnerable samples. First, we establish that margin consistency is a necessary and sufficient condition to use a model’s logit margin as a score for identifying non-robust samples. Next, through comprehensive empirical analysis of various robustly trained models on CIFAR10 and CIFAR100 datasets, we show that they indicate strong margin consistency with a strong correlation between their input space margins and the logit margins. Then, we show that we can effectively use the logit margin to confidently detect brittle decisions with such models and accurately estimate robust accuracy on an arbitrarily large test set by estimating the input margins only on a small subset. Finally, we address cases where the model is not sufficiently margin-consistent by learning a pseudo-margin from the feature representation. Our findings highlight the potential of leveraging deep representations to efficiently assess adversarial vulnerability in deployment scenarios.

## 1 Introduction

Deep neural networks are known to be vulnerable to adversarial perturbations, visually insignificant changes in the input resulting in the so-called adversarial examples that alter the model’s prediction (Biggio et al., 2013; Goodfellow et al., 2015). They constitute actual threats in real-world scenarios (Evtimov et al., 2017; Gnanasambandam et al., 2021), jeopardizing their deployment in sensitive and safety-critical systems such as autonomous driving, aeronautics, and health care. Research in the field has been intense and produced various adversarial training strategies to defend against

the vulnerability to adversarial perturbations with bounded  $\ell_p$  norm (e.g.,  $p = 2$ ,  $p = \infty$ ) through augmentation, regularization, and detection (Xu et al., 2017; Madry et al., 2018; Zhang et al., 2019; Carmon et al., 2019; Wang et al., 2020; Wu et al., 2020; Rice et al., 2020), to cite a few. The empirical robustness (adversarial accuracy) of these adversarially trained models is still far behind their high performance in terms of accuracy. It is typically estimated by assessing the vulnerability of samples of a given test set using adversarial attacks (Carlini & Wagner, 2016; Madry et al., 2018) or an ensemble of attacks such as the standard *AutoAttack* (Croce & Hein, 2020b). The objective of that evaluation is to determine if, for a given normal sample, an adversarial instance exists within a given  $\epsilon$ -ball around it. Yet, this robustness evaluation over a specific test set gives a global property of the model but not a local property specific to a single instance (Seshia et al., 2018; Dreossi et al., 2019). Beyond that particular test set, obtaining this information for each new sample would typically involve rerunning adversarial attacks or performing a formal robustness verification, which in certain contexts may be computationally prohibitive in terms of resources and time. Indeed, in high-stakes deployment scenarios, knowing the vulnerability of single instances in real-time (i.e., their susceptibility to adversarial attacks) would be valuable, for example, to reduce risk, prioritize resources, or monitor operations. Current research lacks efficient and scalable ways to determine the vulnerability of a sample in a deployment context.

The input space margin (i.e., the distance of the sample to the model’s decision boundary in the input space), or input margin in short, can be used as a score to determine whether the sample is non-robust and, as such, likely to be vulnerable to adversarial attacks. Computing the exact input margin is intractable for deep neural networks (Katz et al., 2017; Elsayed et al., 2018; Jordan & Dimakis, 2020). These input margins may not be meaningful for fragile models with zero adversarial accuracies as all samples are vulnerable (close to the decision boundary). However, for robustly trained models, where only certain instances are vulnerable, the input margin is very useful in identifying the critical samples. Previous research studies have explored input margins of deep neural networks during training, focusing on their temporal evolution (Mickisch et al., 2020; Xu et al., 2023), and their exploitation in improving adversarial robustness through instance-reweighting with approximations (Zhang et al., 2020; Liu et al., 2021) and margin maximization (Elsayed et al., 2018; Ding et al., 2020; Xu et al., 2023). However, to the best of our knowledge, no previous research studies the relationship between the input space margin and the logit margin of robustly trained deep classifiers in the context of vulnerability detection.

In this paper, we investigate how the deep representation of robust models can provide information about the vulnerability of any single sample to adversarial attacks. We specifically address whether the logit margin as an approximation of the distance to the decision boundary in the feature space of the deep neural network (penultimate layer) can reliably serve as a proxy of the input margin for vulnerability detection. When this holds, we will refer to the model as being *margin-consistent*. The margin consistency property implies that the model can directly identify instances where its robustness may be compromised simply from a simple forward pass using the logit margin. Fig. 1 illustrates this idea of margin consistency. The following contributions are presented in the paper:

- We introduce the notion of *margin consistency*<sup>1</sup>, a property to characterize robust models that allow using their logit margin as a proxy estimation for the input space margin in the context of non-robust sample detection. We prove that margin consistency is a necessary and sufficient condition to reliably use the logit margin for detecting non-robust samples.
- Through an extensive empirical investigation of pre-trained models on CIFAR10 and CIFAR100 with various adversarial training strategies, mainly taken from *RobustBench* (Croce et al., 2021), we provide evidence that almost all the investigated models display strong margin consistency, i.e., there is a strong correlation between the input margin and the logit margin.
- We confirm experimentally that models with strong margin consistency perform well in detecting samples vulnerable to adversarial attacks based on their logit margin. In contrast, models with weaker margin consistency exhibit poorer performance. Leveraging margin consistency, we can also estimate the robust accuracy on an arbitrarily large test set by estimating the input margins only on a small subset.
- For models where margin consistency does not hold, exhibiting a weak correlation between the input margin and the logit margin, we simulate margin consistency by learning to map the model’s feature representation to a pseudo-margin with a better correlation through a simple learning scheme.

---

<sup>1</sup>Code available at: <https://github.com/ngnawejonas/margin-consistency>

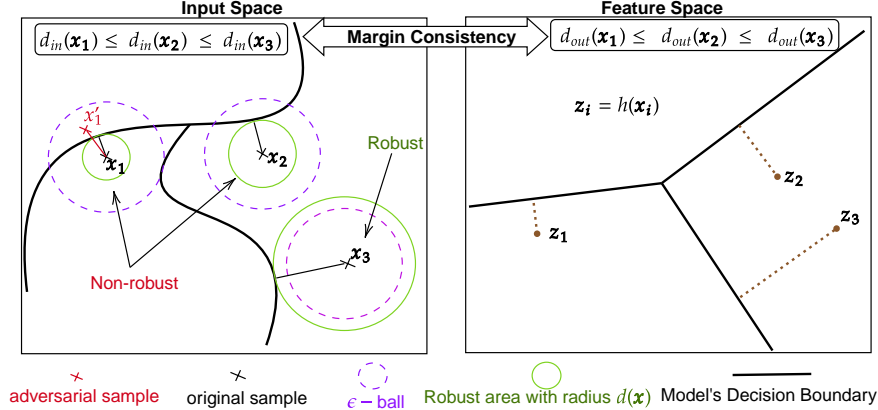


Figure 1: Illustration of the input space margin, margin in the feature space and margin consistency. The margin-consistent model preserves the relative position of samples to the decision boundary in the input space to the feature space.

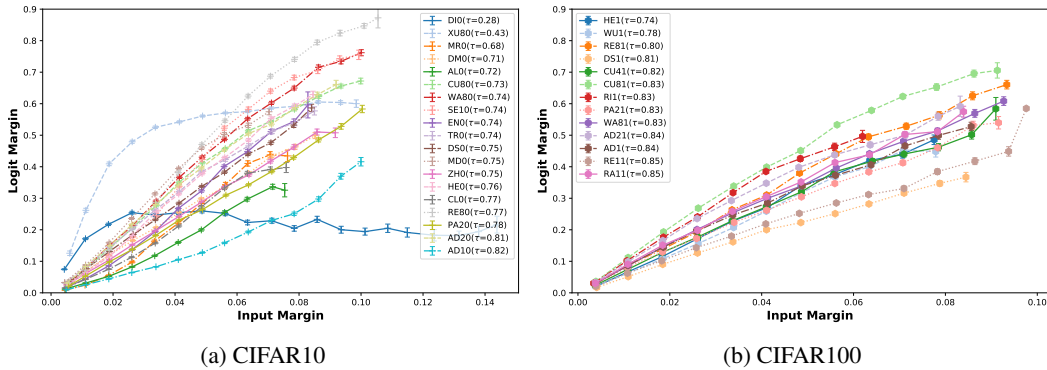


Figure 2: Margin consistency of various models: there is a strong correlation between input space margin and logit margin for most  $\ell_\infty$  robust models tested, the exceptions being **DIO** and **XU8** on CIFAR10. See Table 1 for the references on the models. The plots are given with standard error for the y-axis values in each interval.

## 2 Methodology

### 2.1 Notation and Preliminaries

**Notation** We consider  $f_\theta : \mathbb{R}^n \rightarrow \mathbb{R}^C$  a deep neural network classifier with weights  $\theta$  trained on a dataset of samples drawn iid from a distribution  $\mathcal{D}$  on a product space  $\mathcal{X} \times \mathcal{Y}$ . Each sample  $\mathbf{x}$  in the input space  $\mathcal{X} \subset \mathbb{R}^n$  has a unique corresponding label  $y \in \mathcal{Y} = \{1, 2, \dots, C\}$ . The prediction of  $\mathbf{x}$  is given by  $\hat{y}(\mathbf{x}) = \arg \max_{j \in \mathcal{Y}} f_\theta^j(\mathbf{x})$ , where  $f_\theta^j(\mathbf{x})$  is the  $j$ -th component of  $f_\theta(\mathbf{x})$ . We consider that a deep neural classifier is composed of a feature extractor  $h_\psi : \mathcal{X} \rightarrow \mathbb{R}^m$  and a linear head with  $C$  linear classifiers  $\{\mathbf{w}_j, b_j\}$  such that  $f_\theta^j(\mathbf{x}) = \mathbf{w}_j^\top h_\psi(\mathbf{x}) + b_j$ . The predictive distribution  $p_\theta(y|\mathbf{x})$  is obtained by taking the softmax of the output  $f_\theta(\mathbf{x})$ . A perturbed sample  $\mathbf{x}'$  can be obtained by adding a perturbation  $\delta$  to  $\mathbf{x}$  within an  $\epsilon$ -ball  $B_p(\mathbf{x}, \epsilon)$ , an  $\ell_p$ -norm ball of radius  $\epsilon > 0$  centered at  $\mathbf{x}$ ;  $B_p(\mathbf{x}, \epsilon) := \{\mathbf{x}' : \|\mathbf{x}' - \mathbf{x}\|_p = \|\delta\|_p < \epsilon\}$ . The distance  $\|\mathbf{x}' - \mathbf{x}\|_p = \|\delta\|_p$  represents the perturbation size defined as  $(\sum_{i=1}^n |\delta_i|^p)^{\frac{1}{p}}$ . In this paper, we will focus on  $\ell_\infty$  norm ( $\|\mathbf{x}\|_\infty = \max_{i=1, \dots, n} |x_i|$ ), which is the most commonly used norm in the literature.

**Local robustness** Different notions of **local robustness** exist in the literature (Gourdeau et al., 2021; Zhong et al., 2021; Han et al., 2023). In this paper, we equate local robustness to  $\ell_p$ -**robustness**, a standard notion corresponding to the invariance of the decision within the  $\ell_p$   $\epsilon$ -ball around the sample (Bastani et al., 2016; Fawzi et al., 2018) and formalized in terms of  $\epsilon$ -robustness.

**Definition 1.** A model  $f$  is  $\epsilon$ -robust at point  $\mathbf{x}$  if for any  $\mathbf{x}' \in B_p(\mathbf{x}, \epsilon)$  ( $\mathbf{x}'$  in the  $\epsilon$ -ball around  $\mathbf{x}$ ), we have  $\hat{y}(\mathbf{x}') = \hat{y}(\mathbf{x})$ .

For a given robustness threshold  $\epsilon$ , a data instance is said to be non-robust for the model if this model is not  $\epsilon$ -robust on it. This means it is possible to construct an adversarial sample from that instance in its vicinity (i.e., within an  $\epsilon$ -ball distance from the original instance). A vulnerable sample to adversarial attacks is necessarily non-robust. This notion of local robustness can be quantified in the worst-case or, on average, inside the  $\epsilon$ -ball. We focus here on the worst-case measurement given by the input margin, also referred to as the *minimum distortion* or the *robust radius* (Szegedy et al., 2014; Carlini & Wagner, 2016; Weng, 2019)

**The input space margin** is the distance to the decision boundary of  $f$  in the input space. It is the norm of a minimal perturbation required to change the model’s decision at a test point  $\mathbf{x}$ :

$$d_{in}(\mathbf{x}) = \inf\{\|\delta\|_p : \delta \in \mathbb{R}^n \text{ s.t. } \hat{y}(\mathbf{x}) \neq \hat{y}(\mathbf{x} + \delta)\} = \sup\{\epsilon : f \text{ is } \epsilon\text{-robust at } \mathbf{x}\}. \quad (1)$$

An instance  $\mathbf{x}$  is non-robust for a robustness threshold  $\epsilon$  if  $d_{in}(\mathbf{x}) \leq \epsilon$ . Evaluating Eq. 1 for deep networks is known to be intractable in the general case. An upper bound approximation can be obtained using a point  $\mathbf{x}'_0$ , the closest adversarial counterpart of  $\mathbf{x}$  in  $\ell_p$  norm by  $\hat{d}_{in}(\mathbf{x}) = \|\mathbf{x} - \mathbf{x}'_0\|_p$  (see Fig. 1).

**The logit margin** is the difference between the two largest logits. For a sample  $\mathbf{x}$  classified as  $i = \hat{y}(\mathbf{x}) = \arg \max_{j \in \mathcal{Y}} f_{\theta}^j(\mathbf{x})$  the logit margin is defined as  $\left(f_{\theta}^i(\mathbf{x}) - \max_{j, j \neq i} f_{\theta}^j(\mathbf{x})\right) > 0$ . It is an approximation of the distance to the decision boundary of  $f_{\theta}$  in the feature space. The decision boundary in the feature space around  $\mathbf{z} = h_{\psi}(\mathbf{x})$ , the feature representation of  $\mathbf{x}$ , is composed of  $(C - 1)$  linear decision boundaries (hyperplanes)  $\text{DB}_{ij} = \{\mathbf{z}' \in \mathbb{R}^m : \mathbf{w}_i^{\top} \mathbf{z}' + b_i = \mathbf{w}_j^{\top} \mathbf{z}' + b_j\}$  ( $j \neq i$ ). The margin in the feature space is, therefore, the distance to the closest hyperplane, i.e.  $\min_{j, j \neq i} d(\mathbf{z}, \text{DB}_{ij})$ , where the distance  $d(\mathbf{z}, \text{DB}_{ij})$  from  $\mathbf{z}$  to a hyperplane  $\text{DB}_{ij}$  has a closed-form expression:

$$d(\mathbf{z}, \text{DB}_{ij}) = \inf\{\|\eta\|_p : \eta \in \mathbb{R}^m \text{ s.t. } \mathbf{z} + \eta \in \text{DB}_{ij}\} = \frac{f_{\theta}^i(\mathbf{x}) - f_{\theta}^j(\mathbf{x})}{\|\mathbf{w}_i - \mathbf{w}_j\|_q}, \quad (2)$$

where  $\|\cdot\|_q$  is the dual norm of  $p$ ,  $q = \frac{p}{p-1}$  for  $p > 1$  (Moosavi-Dezfooli et al., 2016; Elsayed et al., 2018).

When the classifiers  $\mathbf{w}_j$  are equidistant ( $\|\mathbf{w}_i - \mathbf{w}_j\|_q = \omega > 0, \forall i, j$ ), the margin becomes:

$$\min_{j, j \neq i} \frac{f_{\theta}^i(\mathbf{x}) - f_{\theta}^j(\mathbf{x})}{\omega} = \frac{1}{\omega} \min_{j, j \neq i} \left(f_{\theta}^i(\mathbf{x}) - f_{\theta}^j(\mathbf{x})\right) = \frac{1}{\omega} \underbrace{\left(f_{\theta}^i(\mathbf{x}) - \max_{j, j \neq i} f_{\theta}^j(\mathbf{x})\right)}_{\text{logit margin}}. \quad (3)$$

Under the equidistance assumption, the logit margin is proportional (equal up to a scaling factor) to the margin in the feature space. We will denote the logit margin of  $\mathbf{x}$  by  $d_{out}(\mathbf{x})$ :

$$d_{out}(\mathbf{x}) = f_{\theta}^i(\mathbf{x}) - \max_{j, j \neq i} f_{\theta}^j(\mathbf{x}) \quad (4)$$

## 2.2 Margin Consistency

**Definition 2.** A model is *margin-consistent* if there is a monotonic relationship between the input space margin and the logit margin, i.e.,  $d_{in}(\mathbf{x}_1) \leq d_{in}(\mathbf{x}_2) \Leftrightarrow d_{out}(\mathbf{x}_1) \leq d_{out}(\mathbf{x}_2), \forall \mathbf{x}_1, \mathbf{x}_2 \in \mathcal{X}$ .

A margin-consistent model preserves the relative position of samples to the decision boundary from the input space to the feature space. A sample further from (closer to) the decision boundary in the input space remains further from (closer to) the decision boundary in the feature space with respect to other samples, as illustrated in Fig. 1.

We can evaluate margin consistency by computing the **Kendall rank correlation** ( $\tau \in [-1, 1]$ ) between the output scores and the input margins over a test set. The Kendall rank correlation tests the existence and strength of a monotonic relationship between two variables. It makes no assumption on the distribution of the variables and is robust to outliers (Chattamvelli, 2024). Perfect margin consistency corresponds to an absolute value of 1, and 0 means the absence of margin consistency.

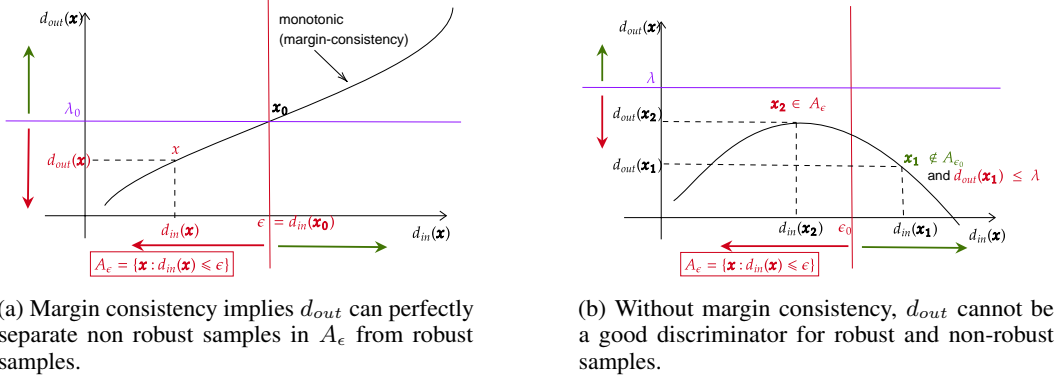


Figure 3: Illustration of Theorem 1’s proof.

### 2.3 Non-robust Samples Detection

Non-robust detection can be defined as a scored-based binary classification task where non-robust samples constitute the positive class, and the input margin  $d_{in}$  induces a perfect discriminative function  $g$  for that:

$$g(\mathbf{x}) = \mathbb{1}_{[d_{in}(\mathbf{x}) \leq \epsilon]}(\mathbf{x}) = \begin{cases} 1 & \text{if } \mathbf{x} \text{ is non-robust} \\ 0 & \text{if } \mathbf{x} \text{ is robust} \end{cases}.$$

If a model is margin-consistent, its logit margin can also be a discriminative score to detect non-robust samples. The following theorem establishes that this is a necessary and sufficient condition. Therefore, the degree to which a model is margin-consistent should determine the discriminative power of the logit margin.

**Theorem 1.** *If a model is margin-consistent, then for any robustness threshold  $\epsilon$ , there exists a threshold  $\lambda$  for the logit margin  $d_{out}$  that separates perfectly non-robust samples and robust samples. Conversely, if for any robustness threshold  $\epsilon$ ,  $d_{out}$  admits a threshold  $\lambda$  that separates perfectly non-robust samples from robust samples, then the model is margin-consistent.*

*Proof sketch.* Fig. 3 presents intuition behind the proof of Theorem 1. For the first part of the theorem (see Fig. 3a), if there is a monotonic relationship between  $d_{in}$  and  $d_{out}$  (margin consistency), any point  $\mathbf{x}$  with  $d_{in}$  less than the threshold  $\epsilon$  (non-robust) will also have  $d_{out}$  less than  $\lambda = d_{out}(\mathbf{x}_0)$  (with  $d_{in}(\mathbf{x}_0) = \epsilon$ ). For the second part (see Fig. 3b), if there are two points  $\mathbf{x}_1$  and  $\mathbf{x}_2$  with non-concordant  $d_{in}$  and  $d_{out}$  (no margin consistency), then for a threshold  $\epsilon_0$  between  $d_{in}(x_1)$  and  $d_{out}(x_2)$ , they will both have different classes but no threshold of  $d_{out}$  (horizontal line) can classify them both correctly. The complete proof of Theorem 1 is deferred to Appendix A.

**Common metrics for detection** include (Hendrycks & Gimpel, 2017; Corbière et al., 2019; Zhu et al., 2023): the Area Under the Receiver Operating Curve (**AUROC**), which ensures the ability of a model to distinguish between the positive and negative classes across all possible thresholds; the Area Under the Precision-Recall Curve (**AUPR**), which evaluates the trade-off between precision and recall and is less sensitive to imbalance between positive and negative classes; and the False Positive Rate (FPR) at a 95% True Positive Rate (TPR) (**FPR@95**), that is crucial in systems where missing positive cases can have serious consequences, such as minimizing the number of vulnerable samples missed. The AUROC and AUPR of a perfect classifier is 1, while 0.5 for a random classifier.

### 2.4 Sample Efficient Robustness Evaluation

Margin consistency enables empirical robustness evaluation over an arbitrarily large test set by only estimating the input margins of a small subset of test samples. For a robustness evaluation at threshold  $\epsilon$  (e.g.,  $\epsilon = 8/255$  in  $\ell_\infty$  norm on CIFAR10 and CIFAR100), we randomly sample a small subset of the large test set and determine the threshold  $\lambda$  for the logit margin that corresponds to  $\epsilon$ . The threshold  $\lambda$  is then used to detect vulnerable samples. With the true labels of these test sets, we can determine the proportion of correct non-vulnerable samples, which is the standard robust accuracy as described in Algorithm 1. A naive way to set the threshold  $\lambda$  at line 6 of Algorithm 1 would be to set it to the detection threshold at  $\alpha = 95\%$  TPR or  $\alpha = 90\%$  TPR, but the logit margin threshold could

---

**Algorithm 1** Sample Efficient Robustness Estimation

---

- 1: **Input:** Test Dataset  $(X, Y) \in (\mathcal{X} \times \mathcal{Y})^N$ , Robustness threshold  $\epsilon > 0$ , Subset size  $n \ll N$ .
  - 2: **Output:** Robust Accuracy Estimation  $\mathcal{A}_r$
  - 3: - Select uniformly at random a subset  $X_n$  of  $n$  samples from  $X$ .
  - 4: - Compute the estimations of the input margins on  $X_n$ ,  $D_n = \{\hat{d}_{in}(\mathbf{x}) : \mathbf{x} \in X_n\}$
  - 5: - Create ground truth labels for vulnerability at threshold  $\epsilon$  i.e.  $\mathbb{1}_{[\hat{d}_{in}(\mathbf{x}) \leq \epsilon]}(\mathbf{x})$ , for  $\mathbf{x} \in X_n$ .
  - 6: - Determine the threshold  $\lambda$  of  $d_{out}$  that gives best approximation of robust accuracy on  $X_n$ .
  - 7: -  $\mathcal{A}_r = |\{\mathbf{x} \in X : d_{out}(\mathbf{x}) > \lambda \text{ and } \hat{y}(\mathbf{x}) = y\}|/N$
- 

vary from one model to another; therefore a better way is to select it by tuning over values  $\alpha \geq 0.80$  that gives the best approximation of the robust accuracy in terms of the absolute error on the small subset  $X_n$ . The same logic applies if we want to estimate the vulnerability of a large dataset without the labels.

### 3 Evaluation

#### 3.1 Experimental Setup

**Datasets and models** We investigate various pre-trained models on CIFAR10 and CIFAR100 datasets. The majority of models were loaded from the *RobustBench* model zoo<sup>2</sup> (Croce et al., 2021), with a few more models that are ResNet-18 (He et al., 2016) models we trained on CIFAR10 with Standard Adversarial Training (Madry et al., 2018), TRADES (Zhang et al., 2019), Logit Pairing (ALP and CLP, Kannan et al. (2018)), and MART (Wang et al., 2020), using the experimental setup of Wang et al. (2020).

**Input margin estimation** This is done using FAB attack (Croce & Hein, 2020a), which is an attack that minimally perturbs the initial instance. Xu et al. (2023) used it in their adversarial training strategy as a reliable way to compute the closest boundary point given enough iterations. We perform the untargeted FAB attack without restricting the distortion to find the boundary for all the samples in the test set instead of constraining the perturbation inside a given  $\epsilon$ -ball when evaluating robustness. As a sanity check for the measured distances, we compare the ratio of correct samples  $\mathbf{x}$  with estimated input margins greater than  $\epsilon = 8/255$  and the robust accuracy in  $\ell_\infty$  norm measured with *AutoAttack* (Croce & Hein, 2020b) at  $\epsilon = 8/255$ . Both quantities estimate the same thing, with a mean and a maximum absolute difference over the models respectively of 1.3 and 6.1 for CIFAR10, 0.48 and 0.75 on CIFAR100, which are reasonable (cf. Fig. 8 in appendix B.1 for the comparison for all the models).

The estimation of the input margins over the 10,000 test samples allows us to create for a given threshold  $\epsilon$  a pool of vulnerable samples that can be successfully attacked at threshold  $\epsilon$  and non-vulnerable samples that were not able to be attacked. Training and distance estimations were run on an NVIDIA Titan Xp GPU (1x).

#### 3.2 Results and Analysis

**Correlation analysis** The results presented in Fig. 2 show that the logit margin has a strong correlation (up to 0.86) with the input margin, which means that they have a level of margin consistency for those models. The plots are given with standard error for the y-axis values in each interval. However, we also observe that two models (i.e., **D10** (Ding et al., 2020) and **XU80** (Xu et al., 2023) WideResNets on CIFAR10) have a weaker correlation. We show in Sec. 3.3 that we can learn to map the feature representation of these models to a pseudo-margin that reflects the distance to the decision boundary in the input space.

**Vulnerable samples detection** We present the results for the robustness threshold  $\epsilon = 8/255$  in Table 1. As expected with the strong correlations, the performance over the non-robust detection task is excellent. We can note that the metrics are lower for the two models with low correlations with

---

<sup>2</sup><https://github.com/RobustBench/robustbench>

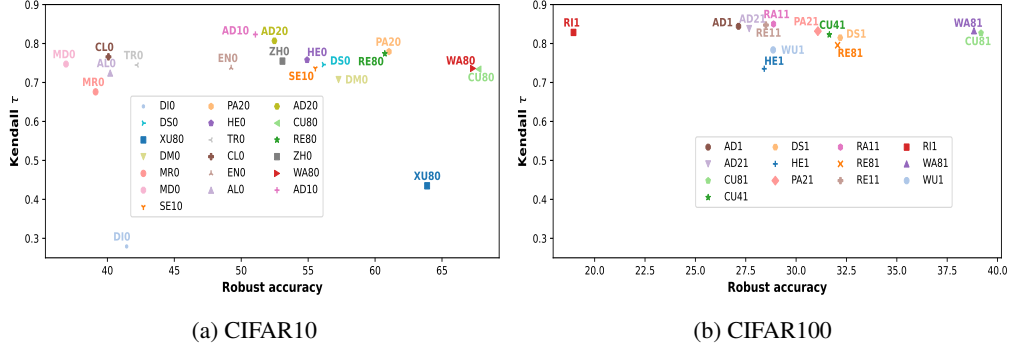


Figure 4: Distribution of the correlation between input margins and logit margins in  $\ell_\infty$  with robust accuracy. The strength of the correlation, which indicates the level of margin consistency, does not depend on the robust accuracy. References on models are given in Table 1.

Model ID	Kendall $\tau$ ( $\uparrow$ )	AUROC ( $\uparrow$ )	AUPR ( $\uparrow$ )	FPR@95 ( $\downarrow$ )	Acc	Rob. Acc	Architecture
<b>CIFAR 10</b>							
DIO (Wu et al., 2020)	0.28	67.49	70.91	82.56	84.36	41.44	WideResNet-28-4
XU80 (Xu et al., 2023)	0.43	83.30	80.50	83.42	93.69	63.89	WideResNet-28-10
MR0 (Wang et al., 2020)	0.68	92.95	94.92	29.76	79.69	39.12	ResNet-18
DM0 (Debenedetti et al., 2023)	0.71	94.31	93.20	32.76	91.30	57.27	XCiT-M12
AL0 (Kannan et al., 2018)	0.72	94.67	95.98	24.93	80.38	40.21	ResNet-18
CU80 (Cui et al., 2023)	0.73	96.87	94.42	17.90	92.16	67.73	WideResNet-28-10
WA80 (Wang et al., 2023)	0.74	96.82	94.33	17.60	92.44	67.31	WideResNet-28-10
SE10 (Sehwag et al., 2021)	0.74	96.03	94.66	19.13	84.59	55.54	ResNet-18
EN0 (Engstrom et al., 2019)	0.74	95.16	95.07	24.10	87.03	49.25	ResNet-50
TR0 (Zhang et al., 2019)	0.74	94.63	96.13	30.93	80.72	42.23	ResNet-18
DS0 (Debenedetti et al., 2023)	0.75	95.80	95.08	24.65	90.06	56.14	XCiT-S12
MD0 (Madry et al., 2018)	0.75	95.36	97.00	23.23	81.85	36.91	ResNet-18
ZH0 (Zhang et al., 2019)	0.75	95.86	95.65	24.91	84.92	53.08	WideResNet-34-10
HE0 (Hendrycks et al., 2019)	0.76	96.35	95.68	20.01	87.11	54.92	WideResNet-28-10
CL0 (Kannan et al., 2018)	0.77	95.93	96.98	20.01	81.12	40.08	ResNet-18
RE80 (Rebuffi et al., 2021)	0.77	97.33	95.70	13.87	87.33	60.73	WideResNet-28-10
PA20 (Pang et al., 2022)	0.78	97.65	96.39	14.40	88.61	61.04	WideResNet-28-10
AD20 (Addepalli et al., 2022)	0.81	97.67	97.46	13.42	85.71	52.48	ResNet-18
AD10 (Addepalli et al., 2021)	0.82	97.86	97.68	13.26	80.24	51.06	ResNet-18
<b>CIFAR 100</b>							
HE1 (Hendrycks et al., 2019)	0.74	94.43	97.39	30.40	59.23	28.42	WideResNet-28-10
WU1 (Wu et al., 2020)	0.78	95.81	98.00	23.34	60.38	28.86	WideResNet-34-10
RE81 (Rebuffi et al., 2021)	0.80	96.87	98.30	18.06	62.41	32.06	WideResNet-28-10
DS1 (Debenedetti et al., 2023)	0.81	96.78	98.30	19.18	67.34	32.19	XCiT-S12
CU41 (Cui et al., 2023)	0.82	97.07	98.48	17.21	64.08	31.65	WideResNet-34-10
CU81 (Cui et al., 2023)	0.83	97.41	98.24	15.62	73.85	39.18	WideResNet-28-10
R11 (Rice et al., 2020)	0.83	96.61	99.05	18.14	53.83	18.95	PreActResNet-18
PA21 (Pang et al., 2022)	0.83	97.66	98.82	13.83	63.66	31.08	WideResNet-28-10
WA81 (Wang et al., 2023)	0.83	97.51	98.28	14.96	72.58	38.83	WideResNet-28-10
AD21 (Addepalli et al., 2022)	0.84	97.46	98.92	16.00	65.45	27.67	ResNet-18
AD1 (Addepalli et al., 2021)	0.84	97.65	98.99	13.88	62.02	27.14	PreActResNet-18
RE11 (Rebuffi et al., 2021)	0.85	97.97	99.05	13.21	56.87	28.50	PreActResNet-18
RA11 (Rade & Moosavi-Dezfooli, 2021)	0.85	98.01	99.08	12.36	61.50	28.88	PreActResNet-18

Table 1: Correlations and vulnerable points detection performance at  $\epsilon = 8/255$  on different adversarially trained models.

particularly very high FPR@95. The performance remains quite good with different values of  $\epsilon$  (cf. appendix B.2).

**Sample Efficient Robustness Estimation** We recover the robust accuracy of the investigated models evaluated with over 10,000 using only a small subset. Fig. 5 shows the absolute error of the estimation for 500 samples. The estimations are still descent with 100 samples (cf. Fig. 10 in appendix B.3).

**Margin Consistency and Lipschitz Smoothness** A neural network  $f$  is said to be  $L$ -Lipschitz if  $\|f(\mathbf{x}_1) - f(\mathbf{x}_2)\| \leq L\|\mathbf{x}_1 - \mathbf{x}_2\|, \forall \mathbf{x}_1, \mathbf{x}_2$ . Lipschitz smoothness is important for adversarial robustness because a small Lipschitz constant  $L$  guarantees the network’s output cannot change more than a factor  $L$  of the change in the input. There are strategies to directly constraint the Lipschitz constant to achieve 1-Lipschitz networks (Cisse et al., 2017; Li et al., 2019; Serrurier et al., 2021; Araujo et al., 2023). Empirical adversarial training strategies aim to achieve Lipschitz’s smoothness indirectly. Note, however, that Lipschitz continuity does not imply margin consistency, for example, two points  $\mathbf{x}_1$  and  $\mathbf{x}_2$  with  $0 < d_{in}(\mathbf{x}_1) < d_{in}(\mathbf{x}_2)$ . While the  $L$ -Lipschitz condition implies that

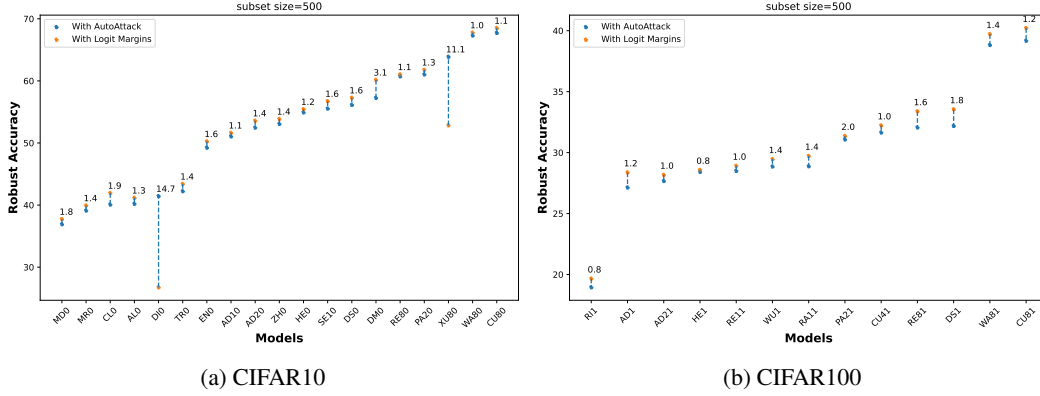


Figure 5: Estimations of the robust accuracy reported by Robustbench using logit margins with only 500 samples are quite accurate both on CIFAR10 and CIFAR100 for strongly margin-consistent models. The numbers indicate the absolute difference between the two values, averaged over ten subsets. See Table 1 for the specific references on the model ID.

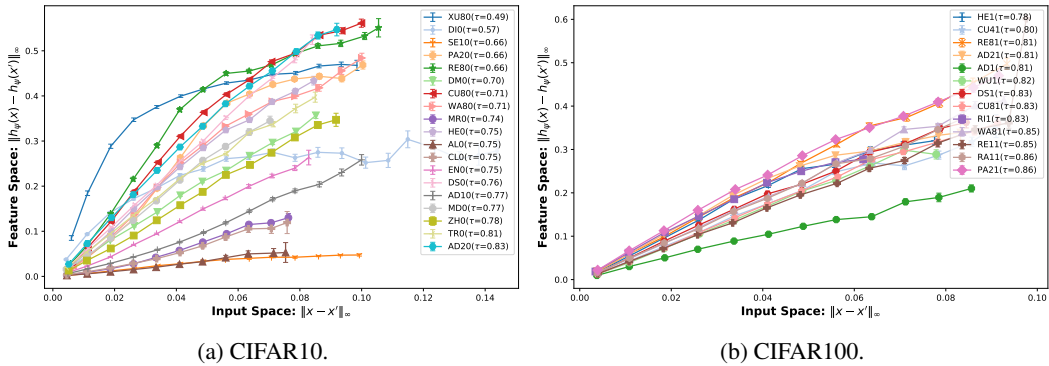


Figure 6: The correlations between the input margin ( $\|\mathbf{x} - \mathbf{x}'\|$ ) and the distance between the feature representations of samples and their adversarial counterparts ( $\|h_{\psi}(\mathbf{x}) - h_{\psi}(\mathbf{x}')\|$ ) suggests a local behaviour of the feature extractor as an isometry (up to a scaling factor). See Table 1 for the specific references on the model ID. The plots are given with standard error for the y-axis values in each interval.

$d_{out}(\mathbf{x}_1) \leq L d_{in}(\mathbf{x}_1)$  for  $i = 1, 2$ , it is clearly possible to have  $d_{out}(\mathbf{x}_2) < d_{out}(\mathbf{x}_1)$ , thus violating the margin consistency condition.

Fig. 4a and 4b show that the strength of the correlation, i.e. the level of margin consistency, does not depend on the robust accuracy.

**Insight into when margin consistency may hold?** We hypothesize that margin consistency can occur when the feature extractor  $h_{\psi}$  behaves locally as an isometry (preserving distances, up to a scaling factor  $\kappa$ ), i.e.,  $\|h_{\psi}(\mathbf{x}) - h_{\psi}(\mathbf{x}')\|_p = \kappa \|\mathbf{x} - \mathbf{x}'\|_p$ . We can experimentally see that there is a high correlation between the input margin ( $\|\mathbf{x} - \mathbf{x}'\|$ ) and the distance between the feature representations of  $\mathbf{x}$  and  $\mathbf{x}'$  (Fig. 6). Given an input sample  $\mathbf{x}$ , by definition  $d_{out}(\mathbf{x}) = \|\mathbf{z} - \mathbf{z}'\|_p$  where  $\mathbf{z} = h_{\psi}(\mathbf{x})$  and  $\mathbf{z}'$  an orthogonal projection of  $\mathbf{z}$  on the boundary hyperplane. The points  $\mathbf{z}$ ,  $\mathbf{z}'$  and  $h_{\psi}(\mathbf{x}')$  will form a right triangle so the side  $\|\mathbf{z} - \mathbf{z}'\|_p$  will directly correlate with side  $\|h_{\psi}(\mathbf{x}) - h_{\psi}(\mathbf{x}')\|_p$ .

### 3.3 Learning a Pseudo-Margin

For the two models that are weakly margin-consistent, we are proposing to directly learn a mapping that maps the feature representation of a sample to a pseudo-margin that reflects the relative position of the samples to the decision in the input space. We use a learning scheme similar to the one



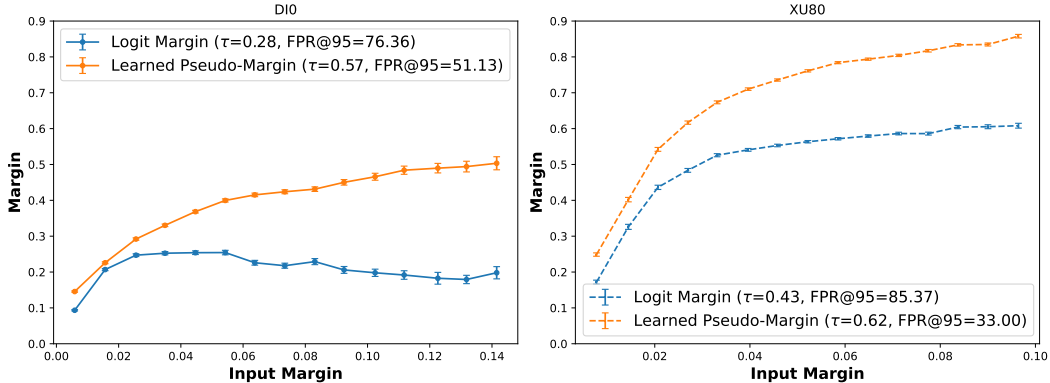


Figure 7: Correlation improvement of the learned pseudo-margin over the logit margin for DI0 (Ding et al., 2020) and XU80 (Xu et al., 2023).

Model ID	Margin	Kendall $\tau$ ( $\uparrow$ )	AUROC ( $\uparrow$ )	AUPR ( $\uparrow$ )	FPR@95 ( $\downarrow$ )	Acc.	Rob. Acc
DI0 (Ding et al., 2020)	Logit margin	0.28	67.49	70.91	82.56	84.36	41.44
	Learned pseudo-margin	<b>0.57</b>	<b>88.49</b>	<b>89.04</b>	<b>51.13</b>		
XU80 (Xu et al., 2023)	Logit margin	0.43	83.30	80.50	83.42	93.69	63.89
	Learned pseudo-margin	<b>0.62</b>	<b>93.66</b>	<b>90.22</b>	<b>33.00</b>		

Table 2: Comparison of the correlation and detection performance between the actual logit margin and the pseudo-margin learned. The models are initially weakly margin-consistent, but the pseudo-margin learned from feature representations simulates the margin consistency with higher correlation and better discriminative power.

of Corbière et al. (2019), with a small ad hoc neural network for learning the confidence of the instances (cf. Fig. 12 in appendix B.4). Given some samples with estimations of their input margins, the objective is to learn to map their feature representation to a pseudo-margin that correlates with the input margins. This learning task can be seen as a learning-to-rank problem. We use a simple learning-to-rank algorithm for that purpose, which is a pointwise regression approach (He et al., 2008) relying on the mean squared error as a surrogate loss.

For the experiment, we used a similar architecture and training protocol as (Corbière et al., 2019) with a fully connected network with five dense layers of 512 neurons, with ReLU activations for the hidden layers and a sigmoid activation at the output layer. We learn using 5000 examples sampled randomly from the training set, with 20% (1000 examples) held as a validation. Fig. 7 and Table 2 show the improved correlation on the learned score compared to the logit margin for both models. The plots are given with standard error for the y-axis values in each interval. The network has learned to recover the relative positions of the samples from the feature representation.

## 4 Related Work

**Detection tasks** in machine learning are found to be of three main types:

- **Adversarial Detection** The goal of adversarial detection (Xu et al., 2017; Carlini & Wagner, 2017) is to discriminate adversarial samples from clean and noisy samples. An adversarial example is a malicious example found by adversarially attacking a sample; it has a different class while being close to the original sample. A vulnerable (non-robust) sample is a normal sample that admits an adversarial example close to it. The two detection tasks are very distinct. Adversarial detection is a defence mechanism like adversarial training; Tramer (2022) has established that both tasks are equivalent problems with the same difficulty.
- **Out-of-Distribution (OOD) detection** In OOD detection (Hendrycks & Gimpel, 2017; Peng et al., 2024), the objective is to detect instances that have a different label from the labels on which the model was trained on. For example, for a model trained on the CIFAR10 dataset, samples from the SVHN dataset are OOD samples for such a model.

- **Misclassification Detection (MisD)** It consists in detecting if the classifier’s prediction is incorrect. This is also referred to as Failure Detection (Corbière et al., 2019) or Trustworthiness Detection (Jiang et al., 2018; Luo et al., 2021). MisD is often used for selective classification (classification with a reject option) (Geifman & El-Yaniv, 2017) to abstain from predicting samples on which the model is likely to be wrong. A score for non-robust detection cannot tell if the sample is incorrect, as a vulnerable sample could be from any side of the decision boundary. Recent work by Mouton et al. (2024) shows that input margins can predict the generalization gap only in specific constrained directions that explain the variance of the training data but not in general.

**Formal robustness verification** aims at certifying whether a given sample is  $\epsilon$ -robust or if it is not an adversarial counter-example can be provided (Brix et al., 2023b). Some complete exact methods based on solving Satisfiability Modulo Theory problems (Katz et al., 2017; Carlini et al., 2017; Huang et al., 2017) or Mixed-Integer Linear Programming (Cheng et al., 2017; Lomuscio & Maganti, 2017; Fischetti & Jo, 2017) provide formal certification given enough time. However, in practice, they are tractable only up to 100,000 activations (Tjeng et al., 2019). Incomplete but effective methods based on linear and convex relaxation methods and Branch-and-Bound methods (Zhang et al., 2018; Salman et al., 2019; Xu et al., 2020, 2021; Zhang et al., 2022; Shi et al., 2023) are faster but conservative, without guaranteed certifications even if given enough time. Scaling them to larger architectures such as WideResNets and large Transformers is still challenging even with GPU acceleration (Brix et al., 2023a; König et al., 2024). Weng et al. (2018) converts the problem of finding the robust radius (input margin) as a local Lipschitz constant estimation problem. Computing the Lipschitz constant of Deep Nets is NP-hard (Virmaux & Scaman, 2018) and Jordan & Dimakis (2020) proved that there is no efficient algorithm to compute the local Lipschitz constant. The estimation provided by Weng et al. (2018) requires random sampling and remains computationally expensive to obtain a good approximation. Vulnerability detection with margin-consistent models does not provide certificates but an empirical estimation of the robustness of a sample as evaluated by adversarial attacks. At scale, it can help filter the samples to undergo formal verification and a more thorough adversarial attack for resource prioritization.

## 5 Limitations and Perspectives

**Vulnerability detection scope** The scope of this work is  $\ell_p$  robustness measured by the input space margin; the minimum distortion that changes the model’s decision while this does not give a full view of the  $\ell_p$  robustness. Samples may be at the same distance to the decision boundary and have unequal unsafe neighbourhoods given an average estimation over the  $\epsilon$ -neighbourhood considered. The average estimation of local robustness for a given  $\epsilon$ -neighborhood remains an open problem, so whether it is possible to extract other notions of robustness from the feature representation efficiently could be a potential avenue for further exploration.

**Attack-based verification** The margin consistency property does not rely on attacks; however, its verification and the learning of a pseudo-margin with an attack-based estimation may not be possible if the model cannot be attacked on sufficient samples. The implicit assumption is that we can always successfully provide the closest point to the decision with a sufficient budget. This is a reasonable assumption since the studied models are not perfectly robust, and the empirical evidence so far with adaptive attacks is that no defence is foolproof, which justifies the need to detect the non-robust samples. In some cases, we might need to combine with an attack such as *CW-attack* (Carlini & Wagner, 2016) to find the closest adversarial sample.

**Influence of terminal phase of training** The work of Pappas et al. (2020) shows that when deep neural network classifiers are trained beyond zero training error and beyond zero cross-entropy loss (aka terminal phase of training), they fall into a state known as *neural collapse*. Neural collapse is a state where the within-class variability of the feature representations collapses to their class means, the class means, and the classifiers become self-dual and converge to a specific geometric structure, an equiangular tight frame (ETF) simplex, and the network classifier converges to nearest train class center. This implies that we may lose the margin consistency property. While neural collapse predicts that all representations collapse on their class mean, in practice, perfect collapse is not quite achieved, and it is precisely the divergence of a representation from its class mean (or equivalently its classifier’s class mean) that encodes the information we seek about the distance to the decision boundary in the input space. Exploring the impact of the neural collapse on margin consistency as models tend toward a collapsed state could provide valuable insights into generalization and adversarial robustness.

## 6 Conclusion

This work addresses the question of efficiently estimating local robustness in the  $\ell_p$  sense at a per-instance level in robust deep neural classifiers in deployment scenarios. We introduce margin consistency as a necessary and sufficient condition to use the logit margin of a deep classifier as a reliable proxy estimation of the input margin for detecting non-robust samples. Our investigation of various robustly trained models shows that they have strong margin consistency, which leads to a high performance of the logit margins in detecting vulnerable samples to adversarial attacks and estimating robust accuracy on arbitrarily large test sets using only a small subset. We also find that margin consistency does not always hold, with some models having a weak correlation between the input margin and the logit margin. In such cases, we show that it is possible to learn to map the feature representation to a better-correlated pseudo-margin that simulates the margin consistency and performs better on vulnerability detection. Finally, we present some limitations of this work, mainly the scope of robustness, the attack-based verification and the impact of neural collapse in terminal phases of training. Beyond its highly practical importance, we see this as a motivation to extend the analysis of robust models and the properties of their feature representations in the context of vulnerability detection.

## Acknowledgements

This work is supported by the DEEL Project CRDPJ 537462-18 funded by the Natural Sciences and Engineering Research Council of Canada (NSERC) and the Consortium for Research and Innovation in Aerospace in Québec (CRIAQ), together with its industrial partners Thales Canada inc, Bell Textron Canada Limited, CAE inc and Bombardier inc.<sup>3</sup>

## References

- Addepalli, S., Jain, S., Sriramanan, G., Khare, S., and Radhakrishnan, V. B. Towards achieving adversarial robustness beyond perceptual limits. In *ICML 2021 Workshop on Adversarial Machine Learning*, 2021. URL [https://openreview.net/forum?id=SHB\\_zn1W5G7](https://openreview.net/forum?id=SHB_zn1W5G7).
- Addepalli, S., Jain, S., Sriramanan, G., and Venkatesh Babu, R. Scaling adversarial training to large perturbation bounds. In *European Conference on Computer Vision*, pp. 301–316. Springer, 2022.
- Araujo, A., Havens, A. J., Delattre, B., Allauzen, A., and Hu, B. A unified algebraic perspective on lipschitz neural networks. In *The Eleventh International Conference on Learning Representations*, 2023. URL <https://openreview.net/forum?id=k71IGLC8cfc>.
- Bastani, O., Ioannou, Y., Lampropoulos, L., Vytiniotis, D., Nori, A., and Criminisi, A. Measuring neural net robustness with constraints. *Advances in neural information processing systems*, 29, 2016.
- Biggio, B., Corona, I., Maiorca, D., Nelson, B., Šrndić, N., Laskov, P., Giacinto, G., and Roli, F. Evasion attacks against machine learning at test time. In *Joint European conference on machine learning and knowledge discovery in databases*, pp. 387–402. Springer, 2013.
- Brix, C., Bak, S., Liu, C., and Johnson, T. T. The fourth international verification of neural networks competition (vnn-comp 2023): Summary and results. *arXiv preprint arXiv:2312.16760*, 2023a.
- Brix, C., Müller, M. N., Bak, S., Johnson, T. T., and Liu, C. First three years of the international verification of neural networks competition (vnn-comp). *International Journal on Software Tools for Technology Transfer*, 25(3):329–339, 2023b.
- Carlini, N. and Wagner, D. Adversarial examples are not easily detected: Bypassing ten detection methods. In *Proceedings of the 10th ACM workshop on artificial intelligence and security*, pp. 3–14, 2017.
- Carlini, N. and Wagner, D. A. Towards evaluating the robustness of neural networks. *2017 IEEE Symposium on Security and Privacy (SP)*, pp. 39–57, 2016.

---

<sup>3</sup><https://deel.quebec>

- Carlini, N., Katz, G., Barrett, C., and Dill, D. L. Provably minimally-distorted adversarial examples. *arXiv preprint arXiv:1709.10207*, 2017.
- Carmon, Y., Raghunathan, A., Schmidt, L., Duchi, J. C., and Liang, P. S. Unlabeled data improves adversarial robustness. *Advances in neural information processing systems*, 32, 2019.
- Chattamvelli, R. *Correlation in Engineering and the Applied Sciences: Applications in R*. Springer Nature, 2024.
- Cheng, C.-H., Nührenberg, G., and Ruess, H. Maximum resilience of artificial neural networks. In *Automated Technology for Verification and Analysis: 15th International Symposium, ATVA 2017, Pune, India, October 3–6, 2017, Proceedings 15*, pp. 251–268. Springer, 2017.
- Cisse, M., Bojanowski, P., Grave, E., Dauphin, Y., and Usunier, N. Parseval networks: Improving robustness to adversarial examples. In *International conference on machine learning*, pp. 854–863. PMLR, 2017.
- Corbière, C., Thome, N., Bar-Hen, A., Cord, M., and Pérez, P. Addressing failure prediction by learning model confidence. *Advances in Neural Information Processing Systems*, 32, 2019.
- Croce, F. and Hein, M. Minimally distorted adversarial examples with a fast adaptive boundary attack. In *International Conference on Machine Learning*, pp. 2196–2205. PMLR, 2020a.
- Croce, F. and Hein, M. Reliable evaluation of adversarial robustness with an ensemble of diverse parameter-free attacks. In *International conference on machine learning*, pp. 2206–2216. PMLR, 2020b.
- Croce, F., Andriushchenko, M., Sehwag, V., Debenedetti, E., Flammarion, N., Chiang, M., Mittal, P., and Hein, M. Robustbench: a standardized adversarial robustness benchmark. In *Thirty-fifth Conference on Neural Information Processing Systems Datasets and Benchmarks Track*, 2021. URL <https://openreview.net/forum?id=SSKZPJct7B>.
- Cui, J., Tian, Z., Zhong, Z., Qi, X., Yu, B., and Zhang, H. Decoupled kullback-leibler divergence loss. *arXiv preprint arXiv:2305.13948*, 2023.
- Debenedetti, E., Sehwag, V., and Mittal, P. A light recipe to train robust vision transformers. In *2023 IEEE Conference on Secure and Trustworthy Machine Learning (SaTML)*, pp. 225–253. IEEE, 2023.
- Ding, G. W., Sharma, Y., Lui, K. Y. C., and Huang, R. Mma training: Direct input space margin maximization through adversarial training. In *International Conference on Learning Representations*, 2020. URL <https://openreview.net/forum?id=HkeryxBtPB>.
- Dreossi, T., Ghosh, S., Sangiovanni-Vincentelli, A., and Seshia, S. A. A formalization of robustness for deep neural networks. *arXiv preprint arXiv:1903.10033*, 2019.
- Elsayed, G., Krishnan, D., Mobahi, H., Regan, K., and Bengio, S. Large margin deep networks for classification. *Advances in neural information processing systems*, 31, 2018.
- Engstrom, L., Ilyas, A., Salman, H., Santurkar, S., and Tsipras, D. Robustness (python library), 2019. URL <https://github.com/MadryLab/robustness>.
- Evtimov, I., Eykholt, K., Fernandes, E., Kohno, T., Li, B., Prakash, A., Rahmati, A., and Song, D. Robust physical-world attacks on machine learning models. *arXiv preprint arXiv:1707.08945*, 2(3):4, 2017.
- Fawzi, A., Fawzi, H., and Fawzi, O. Adversarial vulnerability for any classifier. *Advances in neural information processing systems*, 31, 2018.
- Fischetti, M. and Jo, J. Deep neural networks as 0-1 mixed integer linear programs: A feasibility study. *arXiv preprint arXiv:1712.06174*, 2017.
- Geifman, Y. and El-Yaniv, R. Selective classification for deep neural networks. *Advances in neural information processing systems*, 30, 2017.

- Gnanasambandam, A., Sherman, A. M., and Chan, S. H. Optical adversarial attack. In *Proceedings of the IEEE/CVF International Conference on Computer Vision*, pp. 92–101, 2021.
- Goodfellow, I. J., Shlens, J., and Szegedy, C. Explaining and harnessing adversarial examples. In Bengio, Y. and LeCun, Y. (eds.), *3rd International Conference on Learning Representations, ICLR 2015, San Diego, CA, USA, May 7-9, 2015, Conference Track Proceedings*, 2015. URL <http://arxiv.org/abs/1412.6572>.
- Gourdeau, P., Kanade, V., Kwiatkowska, M., and Worrell, J. On the hardness of robust classification. *The Journal of Machine Learning Research*, 22(1):12521–12549, 2021.
- Han, T., Srinivas, S., and Lakkaraju, H. Efficient estimation of local robustness of machine learning models. In *ICML 3rd Workshop on Interpretable Machine Learning in Healthcare (IMLH)*, 2023. URL <https://openreview.net/forum?id=ZGSfAE1Jmp>.
- He, C., Wang, C., Zhong, Y.-X., and Li, R.-F. A survey on learning to rank. In *2008 International Conference on Machine Learning and Cybernetics*, volume 3, pp. 1734–1739. Ieee, 2008.
- He, K., Zhang, X., Ren, S., and Sun, J. Deep residual learning for image recognition. In *Proceedings of the IEEE conference on computer vision and pattern recognition*, pp. 770–778, 2016.
- Hendrycks, D. and Gimpel, K. A baseline for detecting misclassified and out-of-distribution examples in neural networks. In *International Conference on Learning Representations*, 2017. URL <https://openreview.net/forum?id=Hkg4TI9x1>.
- Hendrycks, D., Lee, K., and Mazeika, M. Using pre-training can improve model robustness and uncertainty. In *International conference on machine learning*, pp. 2712–2721. PMLR, 2019.
- Huang, X., Kwiatkowska, M., Wang, S., and Wu, M. Safety verification of deep neural networks. In *International conference on computer aided verification*, pp. 3–29. Springer, 2017.
- Jiang, H., Kim, B., Guan, M., and Gupta, M. To trust or not to trust a classifier. *Advances in neural information processing systems*, 31, 2018.
- Jordan, M. and Dimakis, A. G. Exactly computing the local lipschitz constant of relu networks. *Advances in Neural Information Processing Systems*, 33:7344–7353, 2020.
- Kannan, H., Kurakin, A., and Goodfellow, I. Adversarial logit pairing. *arXiv preprint arXiv:1803.06373*, 2018.
- Katz, G., Barrett, C., Dill, D. L., Julian, K., and Kochenderfer, M. J. Reluplex: An efficient smt solver for verifying deep neural networks. In *Computer Aided Verification: 29th International Conference, CAV 2017, Heidelberg, Germany, July 24-28, 2017, Proceedings, Part I 30*, pp. 97–117. Springer, 2017.
- König, M., Bosman, A. W., Hoos, H. H., and van Rijn, J. N. Critically assessing the state of the art in neural network verification. *Journal of Machine Learning Research*, 25(12):1–53, 2024.
- Li, Q., Haque, S., Anil, C., Lucas, J., Grosse, R. B., and Jacobsen, J.-H. Preventing gradient attenuation in lipschitz constrained convolutional networks. *Advances in neural information processing systems*, 32, 2019.
- Liu, F., Han, B., Liu, T., Gong, C., Niu, G., Zhou, M., Sugiyama, M., et al. Probabilistic margins for instance reweighting in adversarial training. *Advances in Neural Information Processing Systems*, 34:23258–23269, 2021.
- Lomuscio, A. and Maganti, L. An approach to reachability analysis for feed-forward relu neural networks. *arXiv preprint arXiv:1706.07351*, 2017.
- Luo, Y., Wong, Y., Kankanhalli, M. S., and Zhao, Q. Learning to predict trustworthiness with steep slope loss. *Advances in Neural Information Processing Systems*, 34:21533–21544, 2021.
- Madry, A., Makelov, A., Schmidt, L., Tsipras, D., and Vladu, A. Towards deep learning models resistant to adversarial attacks. In *International Conference on Learning Representations*, 2018. URL <https://openreview.net/forum?id=rJzIBfZAb>.

- Mickisch, D., Assion, F., Greßner, F., Günther, W., and Motta, M. Understanding the decision boundary of deep neural networks: An empirical study. *arXiv preprint arXiv:2002.01810*, 2020.
- Moosavi-Dezfooli, S.-M., Fawzi, A., and Frossard, P. Deepfool: a simple and accurate method to fool deep neural networks. In *Proceedings of the IEEE conference on computer vision and pattern recognition*, pp. 2574–2582, 2016.
- Mouton, C., Theunissen, M. W., and Davel, M. H. Input margins can predict generalization too. *Proceedings of the AAAI Conference on Artificial Intelligence*, 38(13):14379–14387, Mar. 2024. doi: 10.1609/aaai.v38i13.29351. URL <https://ojs.aaai.org/index.php/AAAI/article/view/29351>.
- Pang, T., Lin, M., Yang, X., Zhu, J., and Yan, S. Robustness and accuracy could be reconcilable by (proper) definition. In *International Conference on Machine Learning*, pp. 17258–17277. PMLR, 2022.
- Papayan, V., Han, X., and Donoho, D. L. Prevalence of neural collapse during the terminal phase of deep learning training. *Proceedings of the National Academy of Sciences*, 117(40):24652–24663, 2020.
- Peng, B., Luo, Y., Zhang, Y., Li, Y., and Fang, Z. Conjnorm: Tractable density estimation for out-of-distribution detection. In *Proceedings of the International Conference on Learning Representations*, 2024.
- Rade, R. and Moosavi-Dezfooli, S.-M. Helper-based adversarial training: Reducing excessive margin to achieve a better accuracy vs. robustness trade-off. In *ICML 2021 Workshop on Adversarial Machine Learning*, 2021. URL <https://openreview.net/forum?id=BuD2LmNaU3a>.
- Rebuffi, S.-A., Gowal, S., Calian, D. A., Stimberg, F., Wiles, O., and Mann, T. Fixing data augmentation to improve adversarial robustness. *arXiv preprint arXiv:2103.01946*, 2021.
- Rice, L., Wong, E., and Kolter, Z. Overfitting in adversarially robust deep learning. In *International Conference on Machine Learning*, pp. 8093–8104. PMLR, 2020.
- Salman, H., Yang, G., Zhang, H., Hsieh, C.-J., and Zhang, P. A convex relaxation barrier to tight robustness verification of neural networks. *Advances in Neural Information Processing Systems*, 32:9835–9846, 2019.
- Schwag, V., Mahloujifar, S., Handina, T., Dai, S., Xiang, C., Chiang, M., and Mittal, P. Robust learning meets generative models: Can proxy distributions improve adversarial robustness? *arXiv preprint arXiv:2104.09425*, 2021.
- Serrurier, M., Mamalet, F., González-Sanz, A., Boissin, T., Loubes, J.-M., and Del Barrio, E. Achieving robustness in classification using optimal transport with hinge regularization. In *Proceedings of the IEEE/CVF Conference on Computer Vision and Pattern Recognition*, pp. 505–514, 2021.
- Seshia, S. A., Desai, A., Dreossi, T., Fremont, D. J., Ghosh, S., Kim, E., Shivakumar, S., Vazquez-Chanlatte, M., and Yue, X. Formal specification for deep neural networks. In *International Symposium on Automated Technology for Verification and Analysis*, pp. 20–34. Springer, 2018.
- Shi, Z., Jin, Q., Kolter, J. Z., Jana, S., Hsieh, C.-J., and Zhang, H. Formal verification for neural networks with general nonlinearities via branch-and-bound. *2nd Workshop on Formal Verification of Machine Learning (WFVML 2023)*, 2023.
- Szegedy, C., Zaremba, W., Sutskever, I., Bruna, J., Erhan, D., Goodfellow, I. J., and Fergus, R. Intriguing properties of neural networks. In Bengio, Y. and LeCun, Y. (eds.), *2nd International Conference on Learning Representations, ICLR 2014, Banff, AB, Canada, April 14-16, 2014, Conference Track Proceedings*, 2014. URL <http://arxiv.org/abs/1312.6199>.
- Tjeng, V., Xiao, K. Y., and Tedrake, R. Evaluating robustness of neural networks with mixed integer programming. In *International Conference on Learning Representations*, 2019. URL <https://openreview.net/forum?id=HyGIIdRqtm>.

- Tramer, F. Detecting adversarial examples is (nearly) as hard as classifying them. In *International Conference on Machine Learning*, pp. 21692–21702. PMLR, 2022.
- Virmaux, A. and Scaman, K. Lipschitz regularity of deep neural networks: analysis and efficient estimation. *Advances in Neural Information Processing Systems*, 31, 2018.
- Wang, Y., Zou, D., Yi, J., Bailey, J., Ma, X., and Gu, Q. Improving adversarial robustness requires revisiting misclassified examples. In *International Conference on Learning Representations*, 2020. URL <https://openreview.net/forum?id=rkl0g6EFwS>.
- Wang, Z., Pang, T., Du, C., Lin, M., Liu, W., and Yan, S. Better diffusion models further improve adversarial training. In *International Conference on Machine Learning (ICML)*, 2023.
- Weng, T.-W. Proven: Verifying robustness of neural networks with a probabilistic approach - powerpoint presentation. [https://icml.cc/media/Slides/icml/2019/grandball\(11-11-00\)-11-12-15-4739-proven\\_verifyi.pdf](https://icml.cc/media/Slides/icml/2019/grandball(11-11-00)-11-12-15-4739-proven_verifyi.pdf), 2019. (Accessed on 05/23/2023).
- Weng, T.-W., Zhang, H., Chen, P.-Y., Yi, J., Su, D., Gao, Y., Hsieh, C.-J., and Daniel, L. Evaluating the robustness of neural networks: An extreme value theory approach. In *International Conference on Learning Representations*, 2018. URL <https://openreview.net/forum?id=BkUH1MZOb>.
- Wu, D., Xia, S.-T., and Wang, Y. Adversarial weight perturbation helps robust generalization. *Advances in Neural Information Processing Systems*, 33:2958–2969, 2020.
- Xu, K., Shi, Z., Zhang, H., Wang, Y., Chang, K.-W., Huang, M., Kailkhura, B., Lin, X., and Hsieh, C.-J. Automatic perturbation analysis for scalable certified robustness and beyond. *Advances in Neural Information Processing Systems*, 33, 2020.
- Xu, K., Zhang, H., Wang, S., Wang, Y., Jana, S., Lin, X., and Hsieh, C.-J. Fast and Complete: Enabling complete neural network verification with rapid and massively parallel incomplete verifiers. In *International Conference on Learning Representations*, 2021. URL <https://openreview.net/forum?id=nVZtXBI6LNn>.
- Xu, W., Evans, D., and Qi, Y. Feature squeezing: Detecting adversarial examples in deep neural networks. *arXiv preprint arXiv:1704.01155*, 2017.
- Xu, Y., Sun, Y., Goldblum, M., Goldstein, T., and Huang, F. Exploring and exploiting decision boundary dynamics for adversarial robustness. In *The Eleventh International Conference on Learning Representations*, 2023. URL <https://openreview.net/forum?id=aRTKusckByJ>.
- Zhang, H., Weng, T.-W., Chen, P.-Y., Hsieh, C.-J., and Daniel, L. Efficient neural network robustness certification with general activation functions. *Advances in Neural Information Processing Systems*, 31:4939–4948, 2018. URL <https://arxiv.org/pdf/1811.00866.pdf>.
- Zhang, H., Yu, Y., Jiao, J., Xing, E., El Ghaoui, L., and Jordan, M. Theoretically principled trade-off between robustness and accuracy. In *International conference on machine learning*, pp. 7472–7482. PMLR, 2019.
- Zhang, H., Wang, S., Xu, K., Wang, Y., Jana, S., Hsieh, C.-J., and Kolter, Z. A branch and bound framework for stronger adversarial attacks of ReLU networks. In *Proceedings of the 39th International Conference on Machine Learning*, volume 162, pp. 26591–26604, 2022.
- Zhang, J., Zhu, J., Niu, G., Han, B., Sugiyama, M., and Kankanhalli, M. Geometry-aware instance-reweighted adversarial training. *arXiv preprint arXiv:2010.01736*, 2020.
- Zhong, Z., Tian, Y., and Ray, B. Understanding local robustness of deep neural networks under natural variations. In *International Conference on Fundamental Approaches to Software Engineering*, pp. 313–337. Springer, Cham, 2021.
- Zhu, F., Cheng, Z., Zhang, X.-Y., and Liu, C.-L. Openmix: Exploring outlier samples for misclassification detection. In *Proceedings of the IEEE/CVF Conference on Computer Vision and Pattern Recognition*, pp. 12074–12083, 2023.

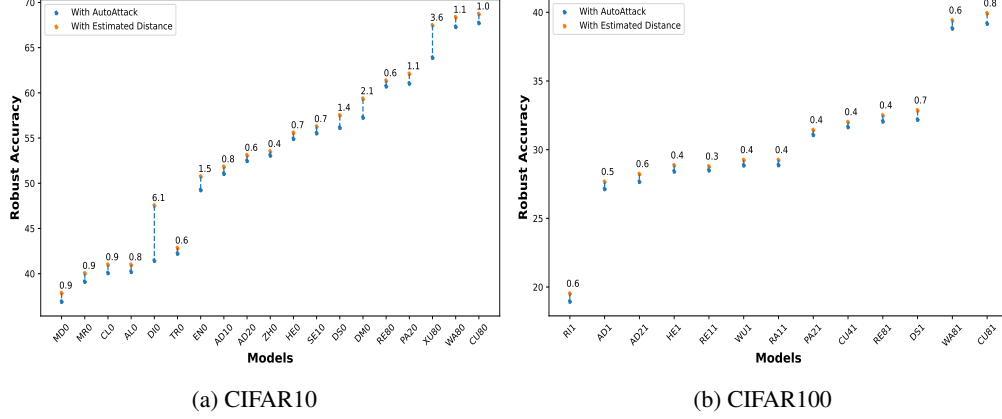


Figure 8: Robust Accuracy reported in Robustbench vs Robust Accuracy estimated with the input margins estimations. They are both close, indicating a good estimation of the input margins.

## A Proof of Theorem 1

**Theorem 1.** *If a model is margin-consistent, then for any robustness threshold  $\epsilon$ , there exists a threshold  $\lambda$  for the logit margin  $d_{out}$  that perfectly separates non-robust samples and robust samples. Conversely, if for any robustness threshold  $\epsilon$ ,  $d_{out}$  admits a threshold  $\lambda$  that perfectly separates non-robust samples from robust samples, then the model is margin-consistent.*

*Proof.* Formally, for a finite sample  $S$  and non-negative values  $\epsilon \geq 0$ ,  $\lambda \geq 0$ , we define:

$$A_\epsilon^S := \{x \in S : d_{in}(\mathbf{x}) \leq \epsilon\} \quad \text{and} \quad B_\lambda^S := \{x \in S : d_{out}(\mathbf{x}) \leq \lambda\}.$$

We say that  $d_{out}$  perfectly separates non-robust samples from robust samples if for any finite sample  $S \subseteq \mathcal{X}$  and every  $\epsilon \geq 0$  there exists  $\lambda \geq 0$  such that  $A_\epsilon^S = B_\lambda^S$ .

**Necessity:** Let's assume that the model is not margin-consistent, i.e., there exist two samples  $\mathbf{x}_1$  and  $\mathbf{x}_2$  such that  $d_{out}(\mathbf{x}_1) \leq d_{out}(\mathbf{x}_2)$  and  $d_{in}(\mathbf{x}_1) > d_{in}(\mathbf{x}_2)$ . By taking  $S = \{\mathbf{x}_1, \mathbf{x}_2\}$  and  $\epsilon = d_{in}(\mathbf{x}_2)$  we have that  $A_\epsilon^S = \{\mathbf{x}_2\}$ . However for any  $\lambda \geq 0$ , if  $\mathbf{x}_2 \in B_\lambda^S$ , then  $d_{out}(\mathbf{x}_1) \leq d_{out}(\mathbf{x}_2) \leq \lambda$  and so  $\mathbf{x}_1 \in B_\lambda^S$ . Therefore  $d_{out}$  does not perfectly separates non-robust samples from robust samples.

**Sufficiency:** Let's assume that the model is margin-consistent. Let  $S$  be a finite sample and consider a threshold  $\epsilon$ . Let  $\mathbf{x}_0$  be the element of the finite set  $A_\epsilon^S$  with maximum  $d_{in}(\mathbf{x}_0)$  and  $d_{out}(\mathbf{x}_0)$ . Since the model is margin-consistent, then for  $\mathbf{x} \in S$ :

$$x \in A_\epsilon^S \Leftrightarrow d_{in}(\mathbf{x}) \leq \epsilon \Leftrightarrow \underbrace{d_{in}(\mathbf{x}) \leq d_{in}(\mathbf{x}_0) \Leftrightarrow d_{out}(\mathbf{x}) \leq d_{out}(\mathbf{x}_0)}_{\text{margin consistency}} \Leftrightarrow d_{out}(\mathbf{x}) \leq \lambda \Leftrightarrow x \in B_\lambda^S.$$

This means we have  $A_\epsilon^S = B_{\lambda_0}^S$ , which shows that  $d_{out}$  perfectly separates non-robust samples from robust samples.  $\square$

## B Supporting Materials

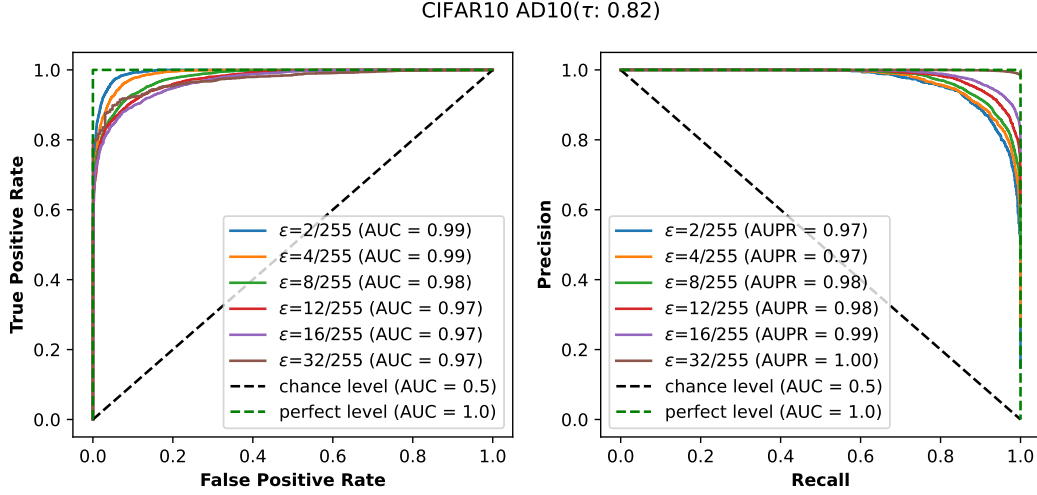
### B.1 Input Margins Estimation Sanity Check

One way to verify the reliability of our estimated input margins is to compare the robust accuracy measured by *AutoAttack* at  $\epsilon = 8/255$  and the proportion of correctly classified test samples with estimated input margins greater than  $\epsilon$ ; both quantities should be approximately equal which happens to be the case –See Fig. 8.

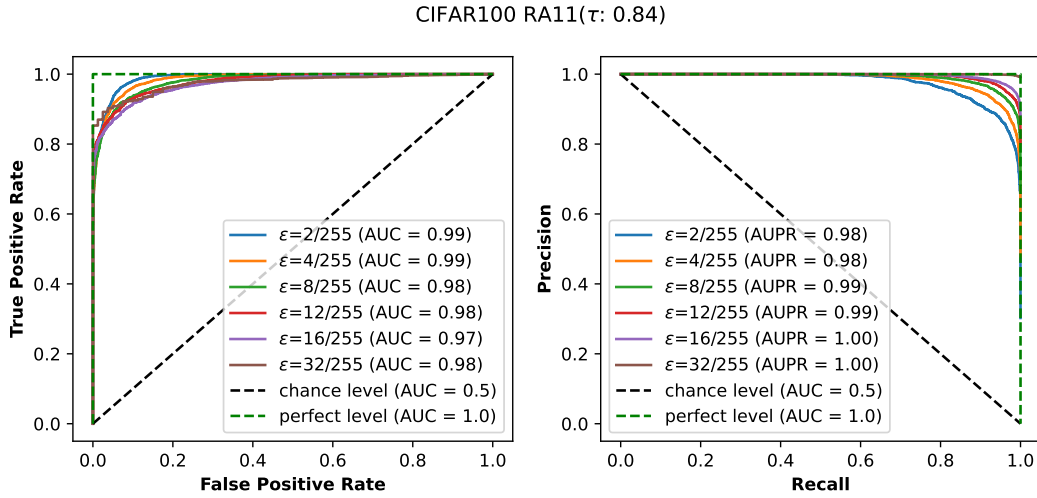
### B.2 Detection Performance at Different Values of $\epsilon$

We present in Fig. 9 the performance of the detection for various values of the robustness threshold. We can see that the strong margin consistency allows the logit margin to be a good proxy for detection





(a) Model **AD10** (Addepalli et al., 2021) on CIFAR10



(b) **RA11** (Rade & Moosavi-Dezfooli, 2021) on CIFAR100

Figure 9: Variation of AUROC score for different values of the threshold  $\epsilon$ .

at various thresholds. Note that below  $\epsilon = 2/255$  and beyond  $\epsilon = 16/255$ , the ratio of vulnerable points to non-vulnerable points becomes too imbalanced, with little to no positive instances beyond  $\epsilon = 32/255$ .

### B.3 Sample Efficient Robust Accuracy Estimation

We plot the variation of the absolute error with subset size for the approximation of the *AutoAttack* Robust Accuracy by the estimation of Algorithm 1. Results are presented in Fig. 10 and Fig. 11 for CIFAR10 and CIFAR100, respectively. From 100 samples, the approximation is already good for some models.

### B.4 Pseudo-margin Learning Setup

The architecture and learning setup for the pseudo-margin is inspired from Corbière et al. (2019). A multilayer perceptron (Fig. 12) learns a pseudo-margin from the feature representations of the samples by minimizing the mean-squared error loss between the output pseudo-margin and an estimation of the input margin.

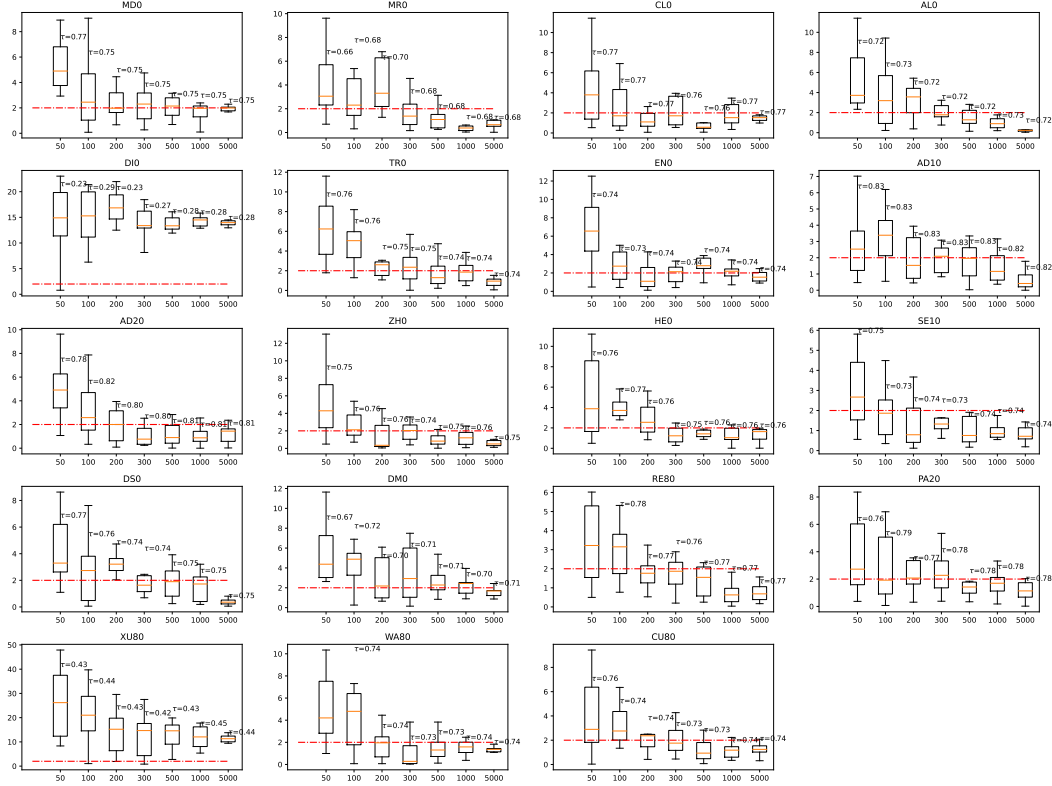


Figure 10: CIFAR10: Variation of the absolute error, with respect to subset size. The results are averaged over 10 variants for each subset size. The Kendall  $\tau$  approximation is also given above the boxplot. The correlation estimation does not vary a lot with sample size. In general, the variance of the absolute error and the value decreases with the increase in subset size. In most cases, the average is already below 2 from 300 samples. The two models with low margin consistency (**DIO** and **XU8**) also have a bad approximation.

## B.5 Verification of Equidistance Assumption of the Linear Classifiers

Eq. 3 in Sec. 2.1 shows that we can approximate the margin in the feature space by the logit margin if the classifiers  $w_j$  are equidistant, i.e.  $\|w_i - w_j\| = C, \forall i, j \in \{1, \dots, C\}$ . For each model, we computed the  $\frac{C(C-1)}{2}$  possible values of the distances between pairs of classifiers (45 for CIFAR10 and 4950 for CIFAR100). We confirm this hypothesis for our investigated models in Fig. 13 by plotting the boxplot of the distribution of values. For each model, the values vary only in a small range.

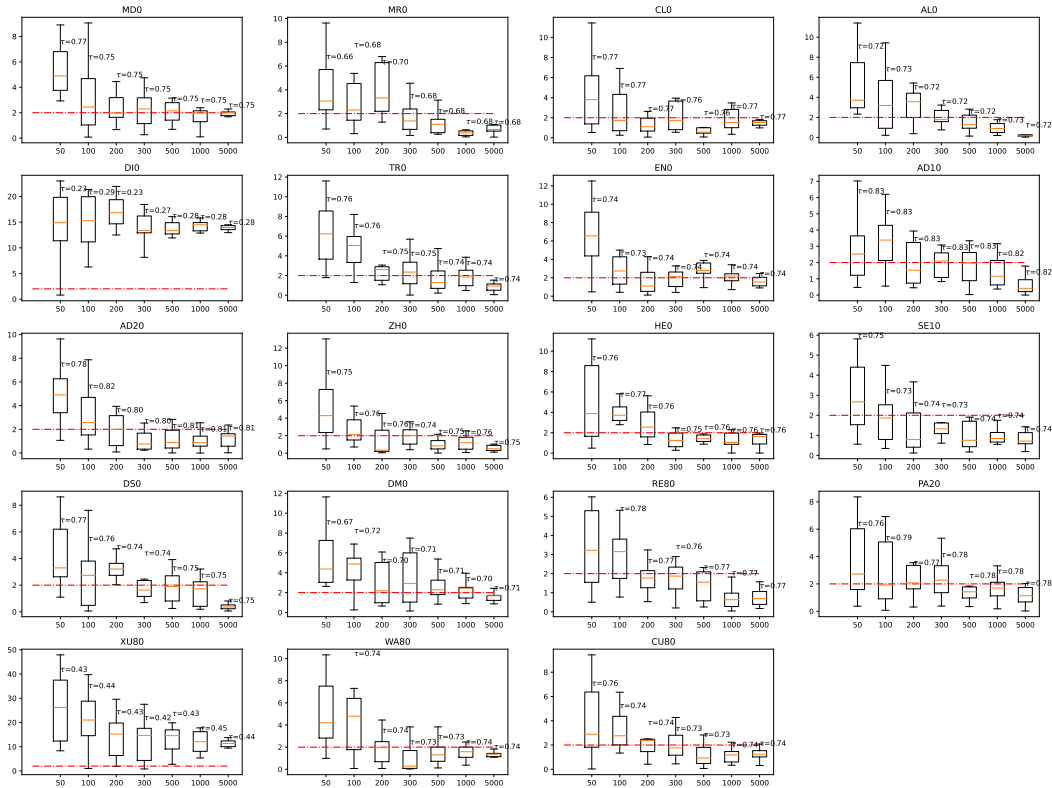


Figure 11: CIFAR100: Variation of the absolute error with respect to subset size. The results are averaged over 10 variants for each subset size. The Kendall  $\tau$  approximation is also given above the boxplot. The correlation estimation does not vary a lot with sample size. In general, the variance of the absolute error and the value decreases with the increase in subset size. In most cases, the average is already below 2 from 300 samples.

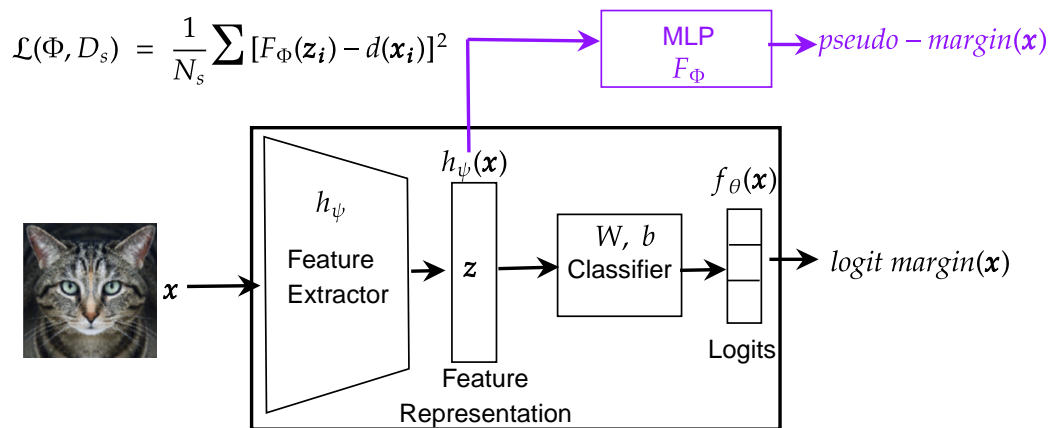


Figure 12: Learning Setup for pseudo-margin inspired from Corbière et al. (2019).

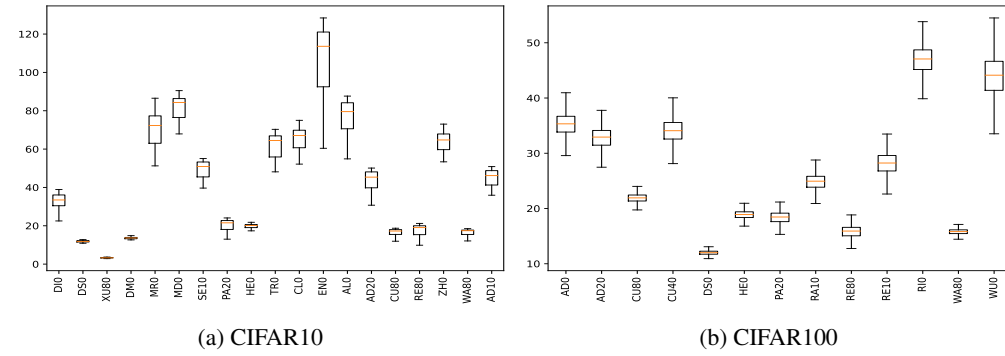


Figure 13: Equidistance of classifiers: the boxplot reports the distances' minimum value, lower quartile ( $Q1$ ), median, upper quartile ( $Q3$ ), and maximum value. The interquartile range is  $Q3 - Q1$  is small enough for most of the models.